Available online at www.sciencedirect.com
ScienceDirect
Journal of Power Sources 169 (2007) 53–58
JOURNAL OF POWER SOURCES
www.elsevier.com/locate/jpowsour

Short communication

Chemical and electrical properties of $BaPr_{0.7}Gd_{0.3}O_{3-\delta}$ ☆

A. Magrasó [a,*], F. Espiell [a], M. Segarra [a], J.T.S. Irvine [b]

[a] *DIOPMA Center, Departament of Materials Science and Metallurgical Engineering, Faculty of Chemistry, University of Barcelona, Martí i Franquès 1, E-08028 Barcelona, Spain*
[b] *School of Chemistry, Purdie Building, University of St. Andrews, Fife KY16 9ST, Scotland, UK*

Available online 30 January 2007

Abstract

Doped perovskites have a growing interest as electrolytes for IT-SOFCs. In the search for proton conducting electrolytes, Gd-doped $BaPrO_3$ was studied. The present work reports the chemical stability and electrical conductivity of $BaPr_{0.7}Gd_{0.3}O_{3-\delta}$ powders. This system is found to be highly reactive under water, CO_2 and hydrogen containing atmospheres. Comparison of the conduction behaviour measured at different atmospheres indicates that the system behaves as a p-type electronic conductor. The total conductivity is about 1×10^{-3} S cm^{-1} at 300 °C, in dry O_2. The resistance of the system seems to be dominated by the grain boundary contribution. However, structure investigation reveals there is a gadolinia segregation, which may act as a resistive barrier. The material is not suitable for SOFC applications due to its low stability.

Keywords: $BaPrO_3$; p-Type conductivity; Proton conductivity; Electrolyte; Electrode; Perovskite

1. Introduction

There is a growing interest on finding new materials susceptible to be used as electrolytes in IT-SOFC, which can reduce the operating temperature to the range under 600 °C. Therefore, energetic costs, chemical degradation and mechanical stress can be reduced.

In that direction, Fukui et al. [1] reported a new perovskite material supposed to be used as proton conducting electrolyte in high temperature proton conducting fuel cells. That material, $BaPr_{1-x}Gd_xO_{3-\delta}$, is very interesting because of its high conductivity (0.1 S cm^{-1} at 500 °C for $x = 0.3$). However, there are still some contradictory results about its nature of conduction. The same author pointed out that the dominant conduction species for the compound $x = 0.4$ used as electrolyte were mainly holes [2]. However, it was later said [3] that compound was not single phase for the mentioned composition and reported a conductivity of 5×10^{-3} S cm^{-1}, $t_{H+} = 0.85$ at 200 °C for $x = 0.3$.

In terms of chemical stability, $BaPrO_3$-based compounds seem to be chemically unstable under CO_2 [3] and under reducing conditions [4]. It has been recently pointed out that $BaPrO_3$ may be also partially reduced under humid conditions [5].

Due to the fact that there is few and contradictory bibliography about $BaPrO_3$ based compounds, in this paper we report a study on the chemical stability of the compound $BaPr_{0.7}Gd_{0.3}O_{3-\delta}$ and the AC impedance studies under various atmospheres.

2. Experimental work

2.1. Sintering studies and morphological characterization

The synthesis of $BaPr_{0.7}G_{0.3}O_{3-\delta}$ was done using the acrylamide combustion synthesis described elsewhere (Magrasó et al. [6]). The sintered bodies were obtained by uniaxial pressing at 3*t*, for 13 mm diameter discs.

A study of the sintering properties of this powder was carried out. The sintering temperature varies from 1250 to 1500 °C and time from 5 up to 30 h. Ramp rate was maintained constant at 3 °C min^{-1} from room temperature.

Because $BaPrO_3$ based compounds react with alumina at high temperatures [3] an old sintered pellet of the same composition was used between the alumina boat and the pellet in order to avoid undesired reactions and consequent stoichiometry losses.

☆ This paper is presented at the 2nd National Congress on Fuel Cells, CONAPPICE 2006.

* Corresponding author. Tel.: +34 93 4021316; fax: +34 93 4035438.
E-mail address: amagraso@ub.edu (A. Magrasó).

0378-7753/$ – see front matter © 2007 Elsevier B.V. All rights reserved.
doi:10.1016/j.jpowsour.2007.01.041

The relative density of the sintered bodies was established by measuring geometrical dimensions. It is considered that Archimedes principle is not accurate enough because liquid media penetrates in the bodies and higher than true density values are found.

Phase identification was carried out in a Phillips PW 1710 X-ray diffractometer to confirm phase purity at high temperatures and check phase decomposition after each thermal treatment under different atmospheres.

SEM was performed with a Leica, Stereoscan 360 microscope (Cambridge instruments, SCT Barcelona) operating at 10 kV in order to check morphology and porosity of the sintered samples.

2.2. TGA studies

TGA analyses were performed in 5% H_2–Ar (wet and dry) to check stability under reducing conditions, and pure O_2 (wet and dry) for oxidizing conditions. The temperature program starts from room temperature up to 700 °C (for H_2) or 900 °C (for O_2), holding at the final temperature for 30 min and then cooling down to room temperature at a flow rate of 20 ml min^{-1} and heating rate of 5 °C min^{-1}.

Also 100% CO_2 TGA analysis were collected to check the stability versus the formation of $BaCO_3$ until 1000 °C, dwelling 120 min at the final temperature.

2.3. Electrical conductivity

A Schlumberger Solartron 1260 Frequency Response Analyser coupled with a 1287 Electrochemical Interface controlled by Zplot electrochemical impedance software was used over the frequency range 3 MHz–1 Hz. AC impedance measurements were made in 25 °C steps (over 100 °C) or 10 °C steps (below 100 °C) in different gas atmospheres between 320 and 50 °C, on dense sintered pellets coated with porous Pt electrodes at both sides. The applied voltage was 0.1 V.

The tested gases have been 5% H_2–Ar and pure O_2. $p(H_2O)$ was modified using dry ($p(H_2O) \approx 3.0 \times 10^{-5}$ atm; bubbling under concentrated solution of H_2SO_4) or wet conditions ($p(H_2O) \approx 2.5 \times 10^{-2}$ atm; bubbling under H_2O). X-ray diffraction was performed after the measurements in order to check possible sample decomposition.

3. Results and discussion

3.1. Sintering studies

A study of the sintering properties of 30GBP powders has been carried out. The summary of the thermal treatment applied and the measured density is displayed in Table 1. The results show that dense bodies (>94% of theoretical density) can be obtained using uniaxial pressing at temperatures above 1400 °C. Five hours are enough as sintering time. A SEM picture of the sintered sample is displayed in Fig. 1. It is possible to observe that the sample looks dense, porosity is not highly present and homogeneous grain size distribution is apparent. X-ray diffraction was carried out after sintering, and the phase could be indexed as *Pbnm* orthorhombic phase, as reported previously [3,6]. However, the phase purity of this material will be discussed later on in the present paper.

Table 1
Summary of theoretical density vs. the different sintering temperature and time

t (h)	T (°C)			
	1250	1300	1400	1500
5	70–80	84–88	89–94	88–94
10	70–80	86–91	93–96	93–96
30	80–85	88–91	93–95	93–95

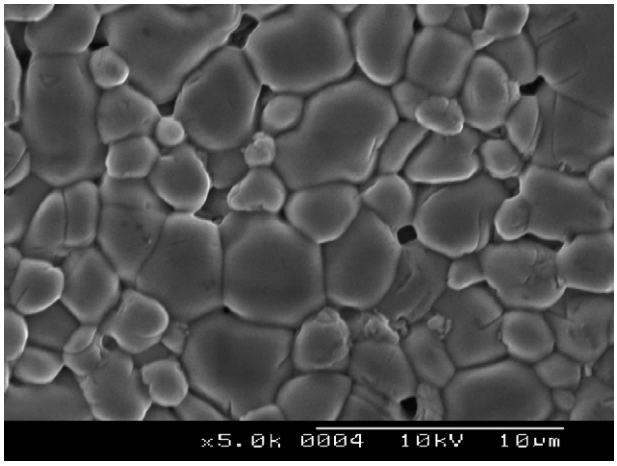

Fig. 1. SEM micrograph of a sintered sample at 1400 °C during 5 h. The relative density of the pellet is 94% of the theoretical.

3.2. Thermal and atmospherical stability

TGA analysis under CO_2 is depicted in Fig. 2. We distinguish three different steps. The first step, between 300 and 630 °C, demonstrates 30GBP incorporates more than 13% its weight in CO_2. This means every mole of 30GBP incorporates more than

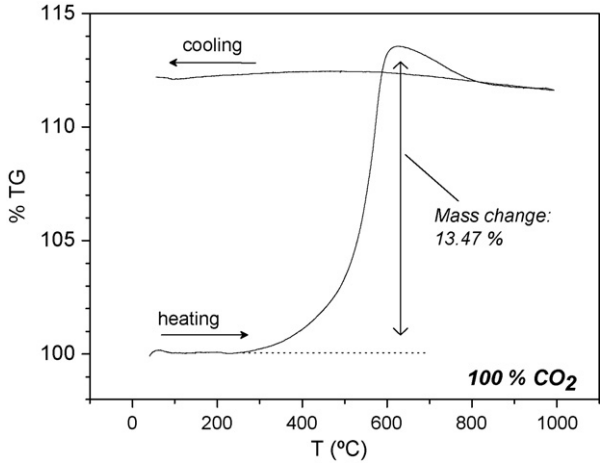

Fig. 2. TGA plot for $BaPr_{0.7}Gd_{0.3}O_{3-\delta}$ run under 100% CO_2 at a rate of 5 °C min^{-1}.

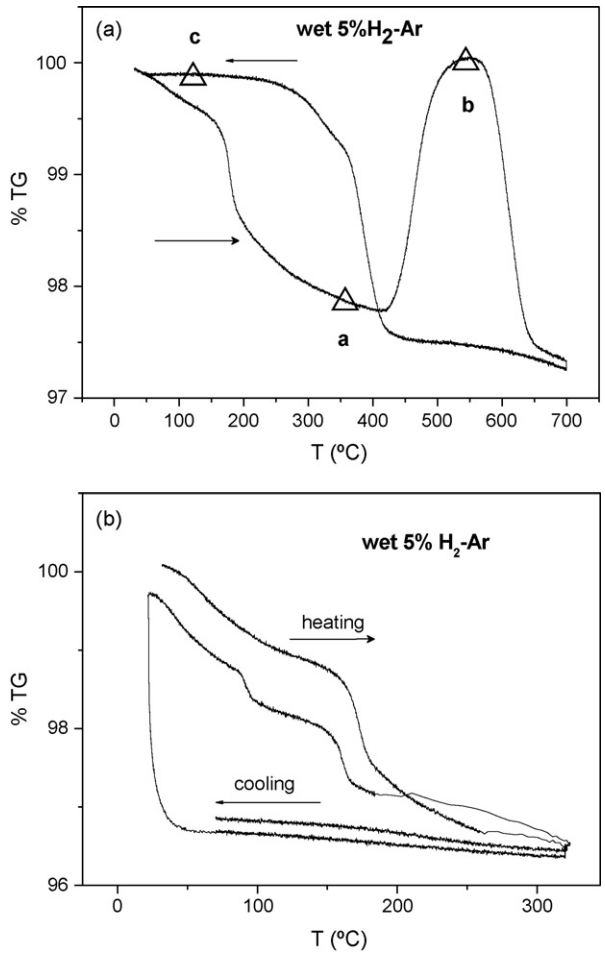

Fig. 3. (a) TGA of 30GBP powder run under wet 5% H_2–Ar. The XRD phase was determined at the points marked as triangles. Decomposition of the sample occurs beyond 420 °C. (b) TGA cycled twice under wet 5% H_2–95% Ar until 320 °C. The final powder was checked by XRD and pure perovskite phase was found.

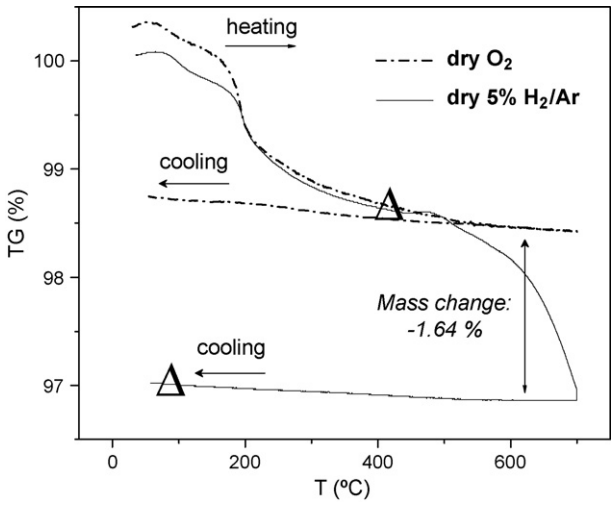

Fig. 4. TGA of the 30GBP sample run under dry 5% H_2–Ar. The XRD phase was determined at the points marked as triangles. *Note*: The samples were not pre-dried before TG measurements.

0.9 moles of CO_2, so nearly all 30GBP phase is decomposed onto barium carbonate and the praseodymium and gadolinium oxides, revealed by XRD. The second step corresponds to a weight loss of about 2% between 630 and 850 °C. It is supposed $BaCO_3$ can react again with the oxides to form the initial 30GBP phase (although not entirely). The final step is practically a plateau in which the decomposed sample does hardly react with the gas. A total CO_2 incorporation over 12% is detected.

30GBP is extremely reactive with CO_2, and X-ray diffraction reveals it is due to the formation of $BaCO_3$. In addition, it was noted that even a dense body slowly reacts with atmospherical CO_2 if it is not kept under inert atmospheres.

The TGA plots in wet 5% H_2–Ar are displayed in Fig. 3. The first weight loss before 200 °C is due to adsorbed water on the surface. Then, an increase of about 2.3% is observed between 420 and 540 °C, which is lost at 620 °C. This step is reversible upon cooling between 450 and 250 °C. This huge weight gain cannot correspond to hydration of $BaPr_{0.7}Gd_{0.3}O_{3-\delta}$ (understood as proton incorporation onto the oxygen vacancies) because the measured weight would involve considerably more oxygen vacancies than those present in the structure. The ratio experimental weight increase/theoretical weight increase is 2.8. This is nearly three times more water than predicted theoretically. X-ray diffraction reveals no perovskite structure at all. The total decomposition of the sample into different hydroxides occurs by point b (Fig. 3(a)). The diffractogram at point c reveals the same transformation as seen by point b. Thus, the big weight changes can be attributed to the reaction of both Pr and Ba to form $Ba(OH)_2{\cdot}nH_2O$ and $Pr(OH)_3$. Besides, it is known that the reaction has some O_2 loss, which cannot be distinguished by TGA measurements. However, even if we counterest the O_2 loss effect on the weight gain we would end up at the same conclusion.

Moreover, an extra experiment was performed in order to find a limit temperature to use 5% H_2 as gas atmosphere for 30GBP samples without decomposing the perovskite structure. A tem-

Table 2
Summary of the final aspect of the powder obtained after the TGA measurements under each atmosphere related to phase purity (referred to pure perovskite phase)

GAS	Dry			Wet		
	Pure phase	Detected impurities	Colour	Pure phase	Detected impurities	Colour
O_2	Yes	–	Initial	No (70% 30GBP)	$Ba(OH)_2{\cdot}nH_2O$, $Pr(OH)_3$	Brown -ash
5% H_2	No (0% 30GBP)	$BaPr_2O_4$ (100%), BaO[a]	Green	No (0% 30GBP)	$Ba(OH)_2{\cdot}nH_2O$, $Pr(OH)_3$	Greenish brown

Initial colour of the perovskite material is dark brown. We must note that Pr^{3+} based compounds tend to form green materials and any colour changes are indicative of Pr reduction.

[a] Difficult to comfirm by XRD as peaks remain broad and small; it might be an amorphous material.

perature well below the decomposition temperature of 30GBP was chosen (320 °C) and then cycling twice at that temperature under wet 5% H_2–Ar; we could observe that the structure was unaltered. The thermogravimetric analysis plot is shown in Fig. 3(b). It was considered that 30GBP is stable under wet 5% H_2 below 320 °C and thus, the electrical characterization of the material under such reducing atmosphere could be tested below that temperature.

The TGA plots under dry O_2 and dry 5% H_2–95% Ar are displayed in Fig. 4. The first step (until 120 °C) is due to adsorbed water on the surface. The second step (120–450 °C) might be due to crystallographic water in the structure. The mentioned water loss is also observed under O_2 containing atmospheres, so it is not due to a reduction process. The theoretical mass loss due to the full reduction of Pr(IV) to Pr (III) (see Eq. (1)) corresponds to an oxygen loss of about 1.70. It is thus in accordance with experimental data (see mass change—1.64% in Fig. 4).

$$BaPr_{0.7}Gd_{0.3}O_{2.85} \rightarrow 0.35BaPr_2O_4 + 0.15BaGd_2O_4 + 0.5BaO + 0.175O_2 \quad (1)$$

The decomposition temperature in dry H_2 is not as clear as for wet H_2, although it starts to occur between 400 and 500 °C, which is similar to the clearer decomposition temperature found in wet-H_2.

The TGA analysis performed under wet O_2 shows a similar trend as dry O_2, although some weight gain of 0.8% is observed on cooling compared to the dehydrated structure. X-ray diffraction was performed after the experiment, and praseodymium and barium hydroxides were identified. Also, some $BaCO_3$ was detected due to rapid reaction between $Ba(OH)_2$ and CO_2. It is thus confirmed that the material is somewhat reactive to water even under oxidizing conditions. The final aspect of the powder obtained after the TGA measurements and the detected impurities under each atmosphere is summarized in Table 2.

3.3. Conductivity

The conductivity measurements of dense sintered 30GBP bodies have been carried out and the stability in different atmospheres has been taken into account to design the experiments.

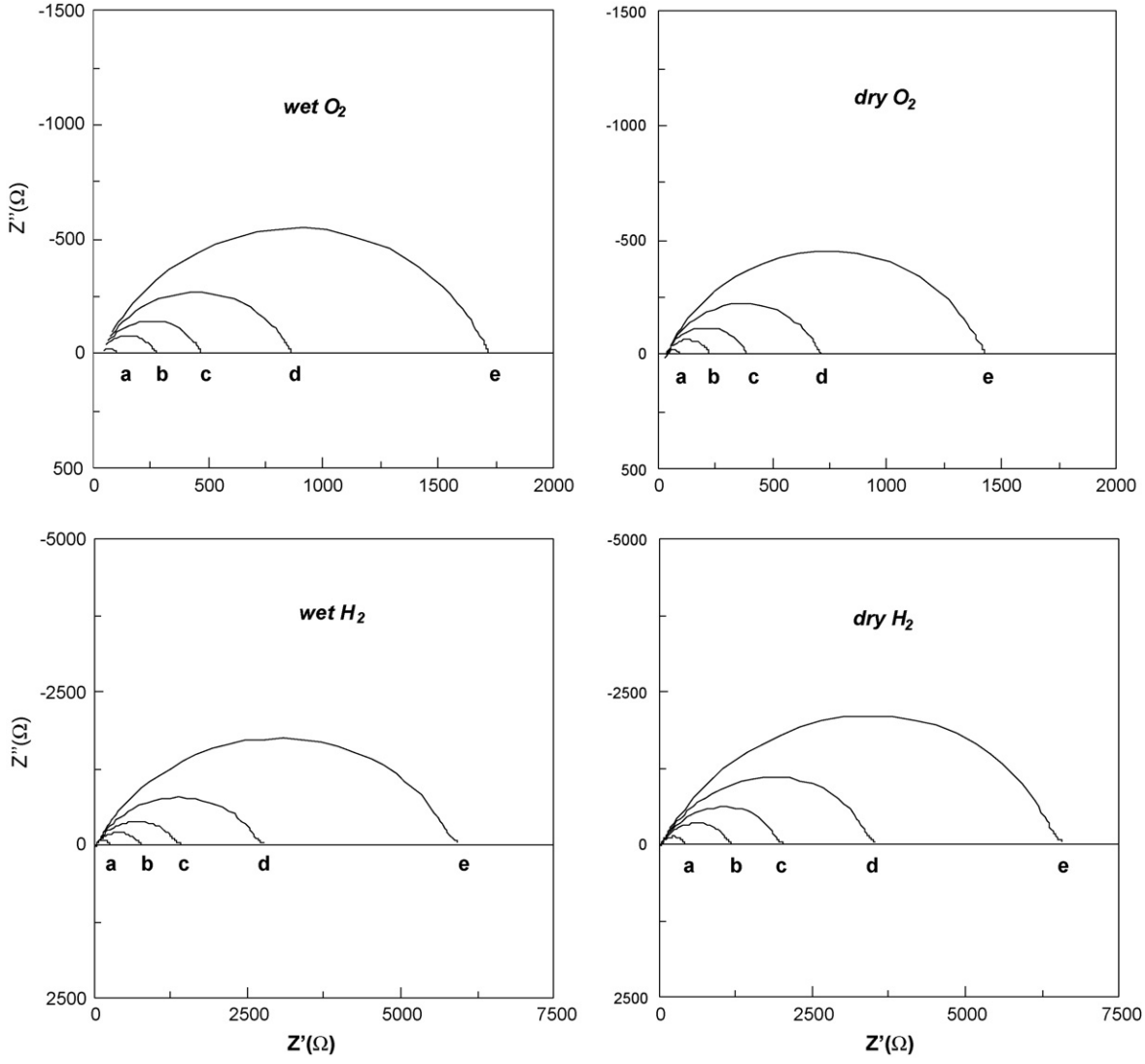

Fig. 5. Nyquist plots of $BaPr_{0.7}Gd_{0.3}O_{3-\delta}$, measured at different atmospheres and temperatures (a, b, c, d and e stand for 300, 250, 225, 200 and 175 °C, respectively).

We concluded in the previous section that dry O_2 does not affect the stability of the material and the sample should remain unreactive under water or reducing conditions if the temperature is kept low enough. The maximum temperature was then set at 320 °C.

AC impedance measurements have been plot using the Zview software. In Fig. 5, the Nyquist representation for typical AC impedance data at all atmospheres are shown. It is possible to observe that the shape of the complex curves is almost unaffected with atmosphere and temperature, being a slightly depressed semicircle with a nearly constant off-set. Of particular interest in the impedance spectra is the relative magnitude of the impedances associated with the bulk crystal lattice and with the grain boundary. This point is critical because the overall ionic conductivity is composed of the sum of these impedances and it is important to know whether the bulk or the grain boundary process dominates, or if they are equal in magnitude. Although the grain boundary component dominates the whole Nyquist plot, it is possible to estimate the bulk contribution from the highest frequency part of the distorted arc as the low frequency intercept of the grain boundary semicircle. Then, it is possible to interpret the AC responses as a R1-R2Q2 circuit. R1 would then be the bulk serial resistance and R2Q2 the grain boundary resistance and the constant phase element, respectively. One may note that the bulk resistance at the lowest temperatures is an indication rather than a true value, because the grain boundary contribution is more than 3 orders of magnitude bigger than the bulk, and therefore, has a lot of associated error. In Fig. 6, one can observe that there is a decrease in total conductivity (mainly grain boundary conductivity) when water is present in the system. Moreover, further tests on the electrical properties of $BaPr_{0.7}Gd_{0.3}O_{3-\delta}$ under wet reducing conditions indicated a considerable reduction of conductivity. Opposite to the behaviour of a typical proton conductor, the fact is rather indicative of a p-type electronic conductor. The total conductivity in dry O_2 was 1×10^{-3} S cm^{-1} and the bulk contribution was approximately 4×10^{-3} S cm^{-1} at

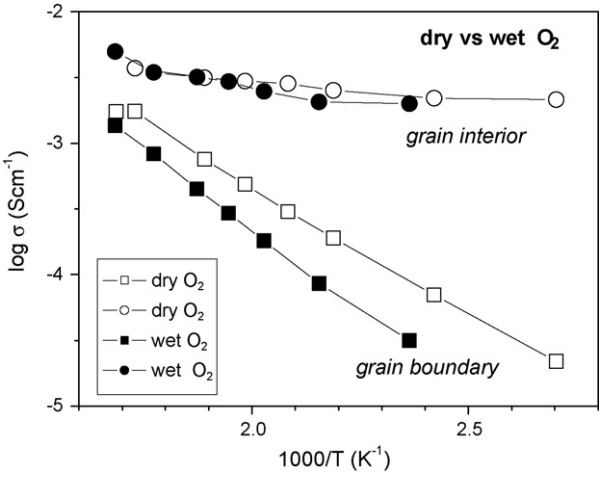

Fig. 6. Arrhenius plots showing bulk and grain boundary contributions in both dry and wet pure O_2. Square points indicate grain boundary conductivity; circular points, bulk conductivity; filled points, wet atmosphere and empty points, dry conditions.

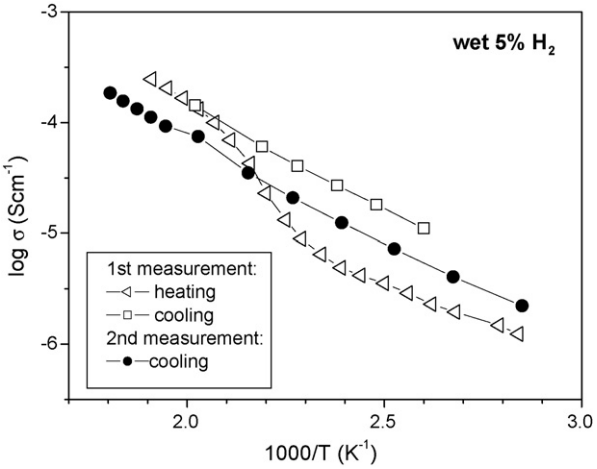

Fig. 7. Arrhenius plot comparing the total electric conductivity of $BaPr_{0.7}G_{0.3}O_{3-\delta}$ under wet 5% H_2–Ar. Hysteresis effect on conduction is found comparing cooling and heating stages.

300 °C. One must say X-ray diffraction revealed a small amount of hydroxides on the surface after measurement, which might be an added factor for the conductivity decrease.

The Arrhenius plot recorded under wet 5% H_2–Ar is shown in Fig. 7. The measurements were repeated twice in order to check the reproducibility. Contrary to what was expected, the loss of conductivity of the second measurement is appreciable, probably occasioned by the degradation of the sample, even if the temperature was kept well below its decomposition temperature under that atmosphere. After the conductivity measurements, XRD patterns on sintered samples after the treatment show the presence of reduced species on the surface. Although the perovskite structure is still a major component, it confirms that the characterization of the material under reducing atmospheres is not possible without avoiding its decomposition.

The capacitance of the grain boundary contribution was calculated using Eq. (2).

$$2\pi f_{\max} RC = 1 \quad (2)$$

The calculated values are of about 3×10^{-9} F under oxidizing conditions and 1×10^{-8} F under reducing conditions. Those are grain boundary capacity values typical of well-sintered samples, which is in accordance with the microstructure observed in Fig. 1.

The effective activation energy for different samples has been calculated for dry oxygen conditions. On the one hand, bulk activation energy is typically around 0.1 eV. Although the calculated conductivity has a lot of associated error, it seems clear that bulk conductivity does not change much with temperature and, thus, very low activation energy values are found. This low number is in accordance with a p-type conductor, more than ionic. On the other hand, grain boundary activation energy depends on the different thermal history of the bodies, but they typically lay between 0.3 and 0.5 eV.

The variation of the structure with temperature and time in $BaPr_{0.7}Gd_{0.3}O_{3-\delta}$ has been carried out by X-ray investigations

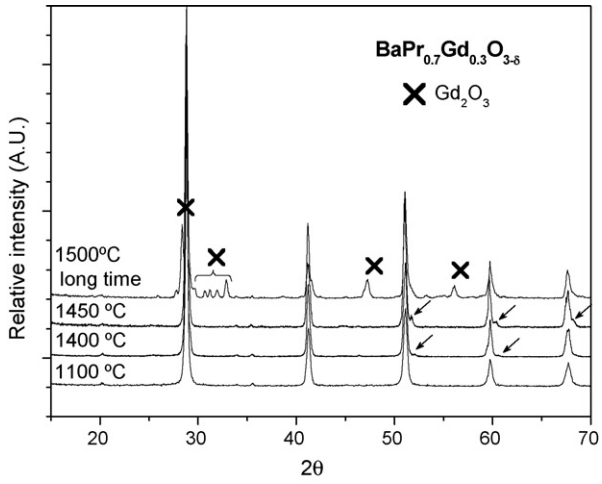

Fig. 8. X-ray diffractograms of $BaPr_{0.7}Gd_{0.3}O_{3-\delta}$ after different thermal treatments. The arrows point an unknown phase which might correspond to a Gd-rich phase.

(Fig. 8). It was found that it suffers an expulsion of gadolinia from the perovskite when long and high temperature thermal treatment is applied. One can observe that small peaks appear at 52.0, 60.2 and 68.2 at "lower" temperature, which later develop onto the segregation of the dopant. These peaks could, in principle, be attributed to the orthorhombic *Pbnm* phase (as it was assumed at the beginning of the present work), but the evolution of the patterns with temperature indicates that those reflections might be due to an unknown gadolinium-rich phase. It remains the possibility that the situation is that we are over the solubility limit of the dopant on the $BaPrO_3$ structure, contrary to what was reported before [3]. This fact would be in accordance with other materials, as a 30% dopant insertion is not a common case among the perovskites.

4. Conclusions

$BaPr_{0.7}Gd_{0.3}O_{3-\delta}$ (30GBP) is an easy material to synthesize and densify up to 94–95% of the theoretical using acrylamide combustion synthesis, simple uniaxial pressing and moderate temperatures (1400–1500 °C). It behaves as a p-type conductor with a total conductivity of 1×10^{-3} S cm^{-1} at 300 °C in dry O_2. It does not behave as a proton conductor.

30GBP is not a stable compound. Barium rapidly reacts with CO_2 to form the correspondent carbonate and Pr(IV) is an element which is easily reduced to Pr (III), in H_2 or even water. High temperature thermal treatment provokes dopant segregation. Therefore, it is not a useful material for SOFC purposes.

Acknowledgements

Authors acknowledge Ministerio de Educación y Ciencia (MAT2003-04556) and BE2004 scholarship (Generalitat de Catalunya) for financial support. We also thank EPSRC for support through a Platform grant. We would also like to thank Sylvia Williamson for TGA and DTA assistance at St. Andrews University and X. Solans (Crystallography Dep., UB) for X-ray data refinement.

References

[1] T. Fukui, S. Ohara, S. Kawatsu, J. Power Sources 71 (1998) 164–168.
[2] T. Fukui, S. Ohara, S. Kawatsu, Solid State Ionics 116 (1999) 331–337.
[3] L. Li, J.R. Wu, S.M. Haile, Electrochem. Soc. Proc. 12 (2001) 214–223.
[4] V.P. Gorelov, B.L. Kuzin, V.B. Balakireva, N.V. Sharova, G.K. Vdovin, S.M. Beresnev, Yu.N. Kleshchev, V.P. Brusentsov, Russ. J. Electrochem. 37 (5) (2001) 505–511.
[5] C.Y. Jones, J. Wu, L. Li, S.M. Haile, J. Appl. Phys. 97 (11) (2005) (114908-1-4).
[6] A. Magrasó, A. Calleja, X.G. Capdevila, F. Espiell, Solid State Ionics 166 (3–4) (2004) 359–364.